ACS Sustainable Chemistry & Engineering

Research Article

Cite This: ACS Sustainable Chem. Eng. 2017, 5, 10342-10351

pubs.acs.org/journal/ascecg

Biodegradable and High-Performance Poly(butylene adipate-*co*-terephthalate)−Lignin UV-Blocking Films

Qianqiu Xing,[†,‡] David Ruch,[‡] Philippe Dubois,[*,‡] Linbo Wu,[*,§] and Wen-Jun Wang[*,†]

[†]State Key Lab of Chemical Engineering, College of Chemical and Biological Engineering, Zhejiang University, 38 Zheda Road, Hangzhou 310027, China

[‡]Department of Materials Research and Technology (MRT), Luxembourg Institute of Science and Technology (LIST), 5 Avenue des Hauts-Fourneaux, L-4362 Esch-sur-Alzette, Luxembourg

[§]Institute of Polymer and Polymerization Engineering, College of Chemical and Biological Engineering, Zhejiang University, 38 Zheda Road, Hangzhou 310027, China

Supporting Information

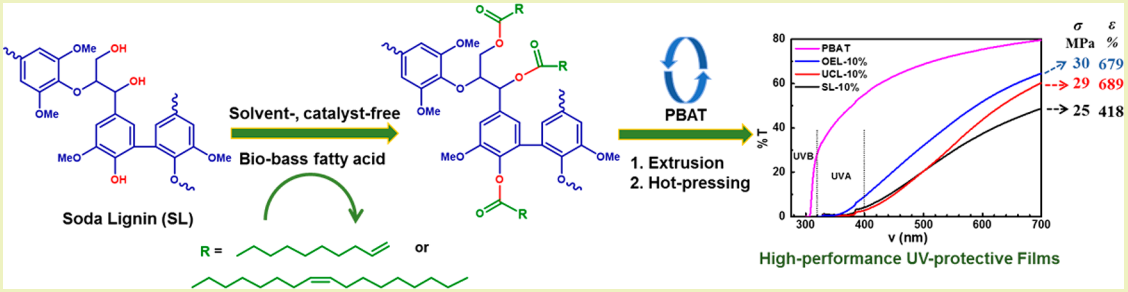

ABSTRACT: Renewable and biodegradable UV-blocking films are in high demand for the increasing need of sustainable environment. Lignin can offer significant UV absorption, but it deteriorates the mechanical properties of films at a high content. In this effort, biobased 10-undecenoic and oleic acids were successfully grafted on soda lignin via solvent- and catalyst-free processes, as confirmed by ^{31}P and ^{1}H NMR and Fourier transform infrared (FTIR). The resulting lignin ester derivatives and neat lignin were then melt-blended with a biodegradable poly(butylene adipate-*co*-terephthalate) (PBAT) to prepare UV-protective films. The incorporation of the modified lignins into the PBAT matrix exhibited good dispersion of lignin particles with almost unaffected tensile properties as well as good thermal stability for up to 20 wt % loading of lignin derivatives. The resulting films showed excellent UV-barrier property with 10 wt % lignin loading, having full protection in the whole UV-irradiation range (280−400 nm). The UV protection of prepared films proved persistent even after UV irradiation for 50 h, and their transparency was evidently enhanced. This work demonstrates a very promising procedure to produce high-performance and biodegradable PBAT−lignin UV-blocking films.

KEYWORDS: *UV-blocking film, Poly(butylene adipate-co-terephthalate), Lignin derivative, Biodegradation, 10-Undecenoic acid, Oleic acid*

INTRODUCTION

Lignin is the second most abundant renewable and biodegradable natural resource on the Earth after cellulose and the main one based on aromatic units.[1,2] Lignin chemical structure originates via an enzyme-mediated dehydrogenative polymerization of phenyl propanoic precursors such as coniferyl, sinapyl, and *p*-coumaryl alcohols,[3] forming a random three-dimensional polymeric network,[4] which may strongly differ depending on the botanical origins.[5] The low-cost lignin production possesses numerous advantages, for example, high carbon content, biodegradability, and antioxidant and antibacterial activities. However, only less than 2% of the approximated 50 million tons of lignin produced from pulping processes per year is employed as high-value products,[6−8] while the rest is simply treated as waste and used in low-value applications, such as for heat and electricity generation.[9] Its brittle nature and incompatibility with other polymer systems are some of the main obstacles in creating lignin-based, high-performance materials. One of the feasible strategies to break the intrinsic constraints of lignin is by chemical modification.[10] In particular, its aliphatic and phenolic hydroxyl (OH) groups can be readily used as a platform for esterification or alkylation, or even for chain extension.[11] The acyl donors generally used in esterification are short-chain fatty acids,[12] while the esterification of lignin with long acyl chain compounds have been utilized to prepare biobased composites of polyethylene (PE) (C_{11}, C_{16}, and C_{18}),[12,13] polypropylene (C_{18}),[14] and polystyrene (C_{18}).[15] The effects of esterification with long fatty acids can significantly lower the glass transition temperature of

Received: July 17, 2017
Revised: September 5, 2017
Published: September 26, 2017

DOI: 10.1021/acssuschemeng.7b02370
ACS Sustainable Chem. Eng. 2017, 5, 10342−10351

lignin esters, even at a low degree of substitution, and improve the melt-flow properties of lignin−polymer blends.[12]

Among the previous studies on lignin polymer composites, those based on biodegradable polymer matrixes are still limited. Lignin acts as an additive in the preparation of starch composite biofilms.[16,17] It has also been blended within polylactic acid (PLA)[18] and used as reinforcement for polybutylene succinate (PBS)[19] and poly(3-hydroxybutyrate-*co*-3-hydroxyvalerate) (PHBV).[20] Poly(butylene adipate-*co*-terephthalate) (PBAT) is a synthetic biodegradable thermoplastic copolyester, possessing comparable mechanical properties to PE.[21] Extensive research and development have been carried out with PBAT in recent decades due to its wide use in applications such as food packaging, agriculture, and biomedical fields.[22,23] Despite the numerous potential applications, its high production costs and poor stability under irradiation, which results in severe deterioration of its mechanical properties, still represent the main limitations, especially for the use of PBAT as a mulching film.[24] Lignin, possessing high UV absorption[25] and low cost, may potentially contribute to elegantly overcome the aforementioned limitations of PBAT. Previous studies reported the effective dispersion of lignin in PBAT, with particle size ranging from ca. 0.4 to 2.5 μm, leading to a retention of toughness and slight improvements in yield stress and tensile modulus.[26] Recently, Sadeghifar et al. prepared cellulose−lignin films, showing that lignin offers significant UV absorption to the films with the drawback of deteriorating the mechanical properties of original cellulose films.[27] Lignin-*g*-PLA copolymers were synthesized and utilized as well-dispersed UV blockers in PLA matrix. However, the tensile properties of the composites with either virgin lignin or modified lignin used at a higher content (4.4 wt %) also decreased compared to neat PLA.[28]

The present work reports for the first time the blending of PBAT with lignin modified with biobased oleic and 10-undecenoic acids. The modification of lignin was achieved under solvent- and catalyst-free conditions, leading to the esterification of both phenolic and aliphatic hydroxyl groups, as confirmed by ^{31}PNMR, ^{1}H NMR, and FTIR. Neat and modified lignins, 10-undecenoyl lignin (UCL) and oleoyl lignin (OEL), were then melt-blended with PBAT, and the resulting composites were processed into thin films by compression molding. The thermal properties of the produced films were characterized by differential scanning calorimetry (DSC) and thermogravimetric analysis (TGA). Optical and mechanical properties, as well as morphology of PBAT−lignin films, were evaluated by UV−vis spectroscopy, tensile testing, and scanning electron microscopy (SEM), respectively. The UV-protection capability of the PBAT−lignin films was investigated, and the UV-blocking stability of films under UV irradiation was also reported.

EXPERIMENTAL SECTION

Materials. Alkaline soda lignin (SL, Protobind 1000) was supplied by Green Value SA (Switzerland). It is a sulfur-free lignin recovered from a mix of wheat straw (*Triticum sp.*) and Sarkanda grass (*Saccharum officiarum*), obtained after extraction and fractionation according to the corresponding patented process.[29] SL is a low-molar-mass lignin with a high degree of condensation and low content in residual ether bonds.[4] The lignin has a M_n of 838 g·mol^{-1} and initial content of OH groups of 5.2 mmol·g^{-1} calculated by ^{31}P NMR according to standard protocol and reported in the previous work of Buono et al.[30] The lignin was used as received without further purification.

Oleoyl chloride (>80%), 10-undecenoic acid (98%), and oxalyl chloride (>98%) were purchased from TCI Europe; ethyl acetate (99.6%, ACS reagent) and methanol (>98%, ACS reagent) were from Fisher Scientific; 2-chloro-4,4,5,5-tetramethyl-1,3,2-dioxaphospholane (95%), chromium(III) acetylacetonate (99.99%), cholesterol (>99%), chloroform-*d* (100%, 99.96 atom % D), and dimethyl sulfoxide-d_6 (100%, 99.96 atom % D) were from Sigma-Aldrich; and tetrahydrofuran (THF) (99.99%) was from Carlo Erba Reagents. All chemicals were used as received without further purification.

Poly(butylene adipate-*co*-terephthalate) (PBAT) pellets (Biocosafe 2003 F) were kindly provided by Xinfu Pharmaceutical Co., Ltd., China. PBAT has a density of 1.26 g·cm^{-3}, a melt index of 3.5 dg·min^{-1} (ISO 1133, 190 °C/2.16 kg), an aromatic-to-adipic molar ratio of 45:55, M_n of 39 700 g·mol^{-1}, and a polydispersity index of 2.9. It was dried in a vacuum oven at 50 °C for 24 h prior to use.

Syntheses. *Chlorination of 10-Undecenoic Acid.* The 10-undecenoic acid (25 g, 135.7 mmol) was placed in a two-necked 250 mL flame-dried, round-bottom flask flushed with argon and charged with a stirring bar. After addition of ethyl acetate (35 mL), the solution was then cooled to 0 °C in a nitrogen atmosphere. An excess of oxalyl chloride (17.5 mL, 203.5 mmol) was then added dropwise at 0 °C in 15 min. The mixture was then kept at 50 °C for an additional 3 h. The excess of oxalyl chloride and solvent were evaporated under vacuum. The 10-undecenoyl chloride was finally obtained in 95% yield as a clear yellow liquid and used without any further purification. ^{1}H NMR (400 MHz, $CDCl_3$, δ (ppm)): 5.80 (1H, m, =C*H*−), 4.96 (2H, m, H_2C=), 2.88 (2H, t, CH_2COCl), 2.04 (2H, m, CH_2CH=CH$_2$), 1.71 (2H, m, CH_2CH$_2$COCl), 1.42−1.21 (10H, aliphatic chain's protons); ^{13}C NMR (400 MHz, CDCl3, δ (ppm)): 173.64 (*C*OCl), 139.02(=CH−), 114.22 (H_2C=), 47.11 (*C*H$_2$COCl), 33.79 (*C*−CH=CH$_2$), 29.19−28.43 (aliphatic saturated carbons), 25.08(CH$_2$CH$_2$CO); IR (cm^{-1}): 3078 (=C−H stretching), 2929 and 2856 (C−H saturated stretching), 1802 (C=OCl stretching), 1641 (C=C stretching), 1443 and 1404 (C−H saturated bending), 994−911 (C−C= stretching), 724 and 681 (=C−H bending).

Functionalization of SL. The SL was esterified by either 10-undecenoyl chloride or oleoyl chloride with 1.0 equiv to the initial amount of hydroxyl groups in SL calculated by ^{31}P NMR (5.2 mmol g^{-1}). The resulting lignin derivatives were named as *10-undecenoyl lignin* (UCL) and *oleoyl lignin* (OEL). These reactions were carried out at 65 °C for 48 h without any solvent and catalyst.[31,32] Methanol (100 mL) was added at the end of the reaction, and the mixtures were stirred for another 30 min to quench the unreacted chlorides. After the solvent was removed under vacuum, the products (UCL and OEL) were dried under vacuum for 24 h and further used without any additional purification. Master batches of ∼40 g of UCL and OEL were prepared.

Film Processing. *Extrusion Step.* The PBAT was extruded with 10 and 20% (w/w) of neat and modified lignins in a twin-screw microcompounder (Xplore 15 cc, DSM, Geleen, Netherlands) with a nitrogen purge. The processing temperature was set at 130 °C, and the screw speed was 100 rpm. In total, 10 g per batch was introduced in the microcompounder for a total extrusion time of 7 min (with recirculation) to produce strands with diameters of 3−5 mm.

Hot-Pressing Step. The extruded strands were cut into 5 mm length pieces and pressed by a Carver 3851-0 hot-press machine (Wabash, U.S.A.) to obtain thin films with thicknesses of 60−90 μm. The plate temperature was set at 140 °C. After melting the PBAT−lignin blends for 5 min and several degassing steps, the samples were pressed into films with a pressure of 250 bar for 5 min and then cooled down to room temperature under pressure with a water circulation within the plates. The extrusion and hot-pressing steps were also conducted on virgin PBAT pellets serving as a blank control group.

Irradiation of the Films. The PBAT-based films were irradiated for 50 h in a Suntest CPS+ chamber (Atlas, Linsengericht, Germany), which made use of a xenon lamp and a solar standard filler (filter according to COLIPA and DIN 67501). The condition of simple daylight 400 W·m^{-2} and black-panel temperature at 63 °C was adopted.

Characterization. *NMR Spectroscopy.* When magnetic resonance techniques were applied to untreated lignin, the resulting spectra were unable to provide its quantitative structural information, as signal overlap occurred between the various types of hydroxyl groups present in lignin. To elucidate the fundamental structural details of lignins, the

DOI: 10.1021/acssuschemeng.7b02370
ACS Sustainable Chem. Eng. 2017, 5, 10342−10351

Scheme 1. Esterification of Soda Lignin (SL) To Yield 10-Undecenoyl Lignin (UCL) and Oleoyl Lignin (OEL)

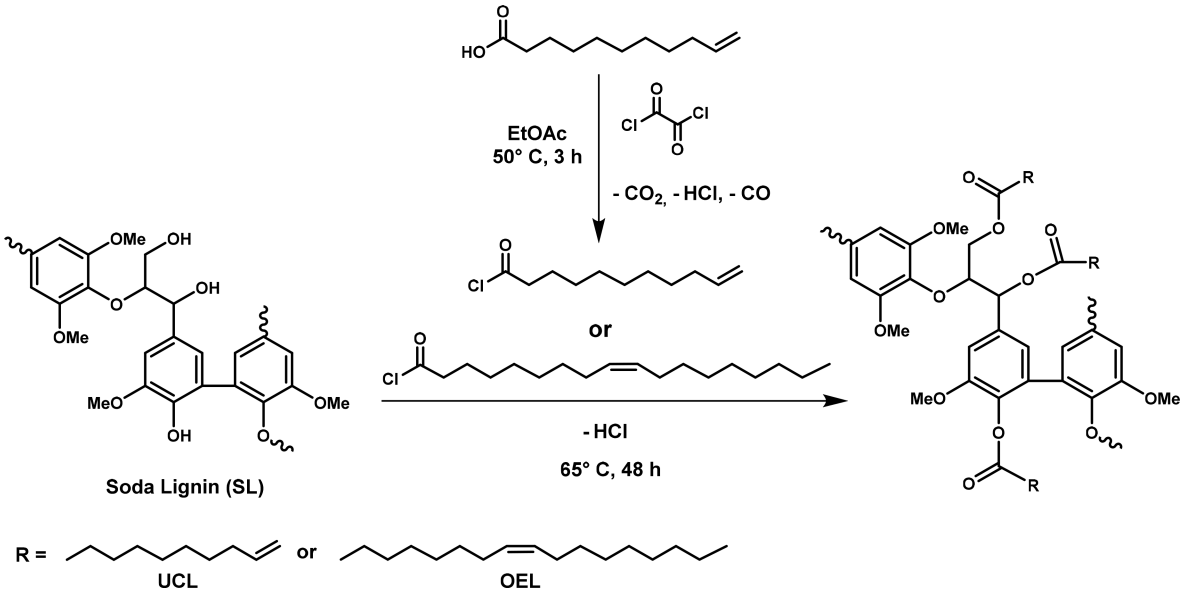

phosphorus reagents were used to derivate their labile protons. The resulting phosphorus-tagged lignin polymers were then measured by the solution phosphorus-31-based NMR methods.[33] In the present work, the ^{31}P NMR analysis was performed on lignin samples phosphytilated with 2-chloro-4,4,5,5-tetramethyl-1,3,2- dioxaphospholane, using cholesterol as internal standard, according to standard protocol.[34] One hundred twenty-eight scans were recorded with a 15 s delay and a spectral width of 80 ppm (180−100 ppm). For quantitative ^{1}H NMR analysis, ∼20 mg of lignin was dissolved in 0.5 mL of dimethyl sulfoxide (DMSO-d_6) before the addition of 100 μL of a standard solution of pentafluorobenzaldehyde (PFB) in DMSO-d_6. All NMR spectra were recorded on a Bruker Ascend 400 MHz spectrometer. Thirty-two scans were collected with a 10 s delay.

FTIR Spectroscopy. FTIR spectroscopy with attenuated total reflectance (ATR) mode was used to characterize the chemical structure of the films. The FTIR-ATR spectra were acquired using a Bruker Tensor 27 (Ettlingen, Germany), over the wavelength range of 4000−400 cm^{-1} with 40 spectral scans.

UV−Vis Absorption Spectroscopy. The UV−vis absorption spectra of SL, UCL, and OEL were performed for 250−700 nm range with a Lambda 35 UV/vis spectrometer (PerkinElmer, Shelton, U.S.A.). For samples with 1,4-dioxane as solvent, the 1,4-dioxane was also scanned at the same wavelength as baseline. The % transparency of the PBAT and PBAT−lignin films in the280−700 nm range was also determined with transmission mode.

Thermogravimetric Analysis Coupled with Mass Spectrometry. The TGA tests of SL, UCL, and OEL were carried out using a STA 409PC Luxx apparatus from NETZSCH (Selb, Germany). The samples, ∼30 mg each, were heated to 800 °C at a heating rate of 10 °C·min^{-1} under argon atmosphere (flow rate = 90 mL·min^{-1}). The evolved species were continuously collected through a heated transfer line to a quadrupole mass spectrometer (NETZSCH Aeolos QMS 403C).

Differential Scanning Calorimetry. The DSC thermograms of all the predried samples were recorded on a TA DSC Q200 calorimeter (TA Instruments). The lignin samples were first heated to 105 °C and maintained at this temperature for 15 min to erase thermal history. They were then cooled to 0 °C, followed by heating to 200 °C. The glass transition temperatures (T_g) were obtained on the second heating run. For PBAT−lignin blends, typical heating/cooling/heating cycles from −70−180 °C at a heating/cooling rate of 10 °C·min^{-1} were used. The T_g and melting temperature (T_m) were collected on the second heating run, while the melt crystallization enthalpy (ΔH_c) was obtained on the cooling run. All the measurements were conducted under nitrogen atmosphere.

Uniaxial Tensile Test. The tensile properties of the film samples were tested under room temperature with an Instron 5967 universal testing machine (Norwood, MA, U.S.A.) according to ASTM D882. They were dried previously in a vacuum oven at 40 °C and successively preconditioned for 48 h under the environmental condition of measurement. At least five dumbbell-shaped specimens of 12.5 mm wide and 75 mm long were tested for each sample. The drawing speed employed was 50 mm·min^{-1}.

Scanning Electron Microscopy. The microstructure of PBAT−lignin composites was investigated using a Quanta FEG 200 environmental scanning electron microscope (FEI, Eindhoven Netherlands). The strands extruded from the microcompounder were cryo-fractured in liquid nitrogen, and their fractured surfaces were observed. The SEM images were obtained at a pressure of 150 Pa, acceleration voltage of 15 kV, and electron beam spot size of 3.0−3.1.

RESULTS AND DISCUSSION

Syntheses and Characterization of Lignin Derivatives.

The OH groups in SL were esterified by either 10-undecenoyl chloride or oleoyl chloride, leading to the formation of pendant hydrophobic aliphatic chains. Similarly to previous reports,[35] the 10-undecenoyl acid was first converted into its corresponding chloride to increase the reactivity (Scheme 1). As the esterification is conducted under solvent- and catalyst-free condition, such a modification can also be applied to the sulfur-containing kraft lignin,[12,13,15] which is much more prevalent than the soda lignin.

The success of the esterification was evidenced by ^{31}P and ^{1}H NMR, as well as by FTIR. As mentioned in the Experimental Section, the ^{31}P NMR measurements were performed on lignin samples previously phosphytilated with 2-chloro-4,4,5,5-tetramethyl-1,3,2-dioxaphospholane, which allowed for determining the overall distribution of hydroxyl groups present in lignin. In the neat SL ^{31}P NMR spectrum (Figure 1), the signals arising at 148.5−145, 144−136.5, and 135.2−133.2 ppm (DMSO-d_6) are assigned to the phosphotriesters of the aliphatic hydroxyl (OH), phenolic (OH), and carboxylic groups of lignin, respectively. The spectra of the modified lignins reveal full disappearance of the aliphatic OH group signals (148.5−145 ppm), indicating complete esterification of the aliphatic OH groups. However, there are still some traces of phenolic signals, indicating a lower

DOI: 10.1021/acssuschemeng.7b02370
ACS Sustainable Chem. Eng. 2017, 5, 10342−10351

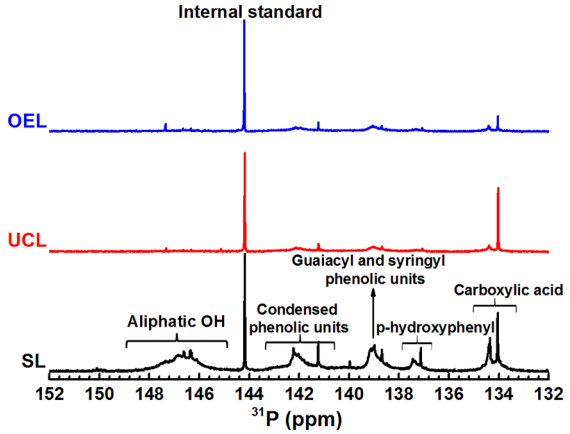

Figure 1. Quantitative ^{31}P NMR spectra of neat lignin (SL), 10-undecenoylated (UCL), and oleoylated (OEL) lignins with signal assignments.

conversion ratio with respect to the values recorded for the aliphatic counterparts.[12,36] These results are in good accordance with the previous study by Buono et al., which reported that ~15% of the aliphatic OH groups could not be accessed, probably because of steric hindrance.[30]

The successful modifications of SL were further confirmed using ^{1}H NMR and FTIR spectroscopy. The ^{1}H NMR (Figure 2a) of OEL shows a strong signal at 5.32 ppm belonging to the C=C double-bond protons (2H, signal a). The methylene groups in oleoyl chain result in signals in the region of 1.25−1.51 ppm (22H, signal b), except for the protons close to the double

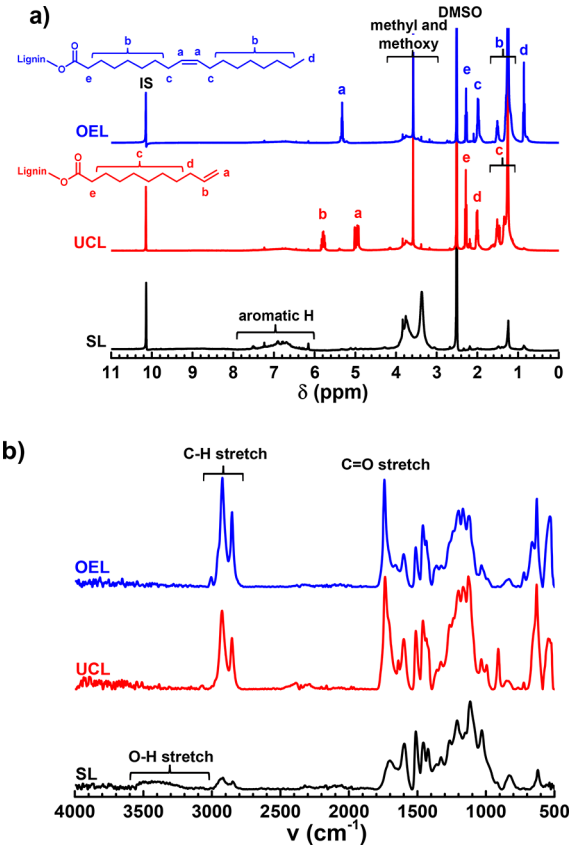

Figure 2. ^{1}H NMR (a) and FTIR (b) spectra of neat (SL), 10-undecenoyl (UCL), and oleoyl (OEL) lignins.

bond appearing at 1.99 ppm (2H, signal c). The terminal chain protons give rise to the signal at 0.86 ppm (3H, signal d), and those in α position to the ester linkage appear at 2.28 ppm (2H, signal e). A similar ^{1}H NMR spectrum is obtained for UCL with the exception of the vinylic protons appearing at 4.95−5.78 ppm and the absence of the terminal CH_3 signal. The double-bond proton's signals are free from overlap with other lignin-related signals and thus were used to quantify the amount of oleoyl and undecenoyl chains grafted, which were 2.09 and 2.38 mmol·g^{-1}, respectively.

Considering the initial content of OH groups in SL and the mass increased by the grafting reaction, the theoretical content of acyl groups (χ_{acyl}) in the resulting derivatives can be calculated by eq 1,

$$\chi_{acyl}(\text{mmol}\cdot\text{g}^{-1}) = \frac{[OH]_{tot}}{1 + [OH]_{tot} \times M_{graftedchain}} \quad (1)$$

where $[OH]_{tot}$ is the total content of OH groups in SL (5.2 mmol·g^{-1}) and $M_{graftedchain}$ refers to the molar mass of the grafted chain, which for oleoyl and undecenoyl chains are 264.37 and 171.28 mg·mmol^{-1}, respectively. The values of χ_{acyl} were calculated to be 2.20 for OEL and 2.79 for UCL, which are quite close to the amounts detected from quantitative ^{1}H NMR analysis.

The FTIR spectra of the modified lignins confirm a complete disappearance of hydroxyl group signals (3000−3600 cm^{-1}), initially present in neat SL (Figure 2b). New absorption bands corresponding to the phenolic and aliphatic carboxylic esters were detected at 1757 and 1740 cm^{-1}, respectively.[37,38] Moreover, the aliphatic C−H stretching at 2851 and 2924 cm^{-1} markedly increased with increasing hydrocarbon chain length. Two additional peaks appeared around 535 and 632 cm^{-1}, which can be assigned to the double bond C−H bending.

The UV−vis spectroscopic properties of SL, UCL, and OEL were measured, and the results are shown in Figure 3. Compared

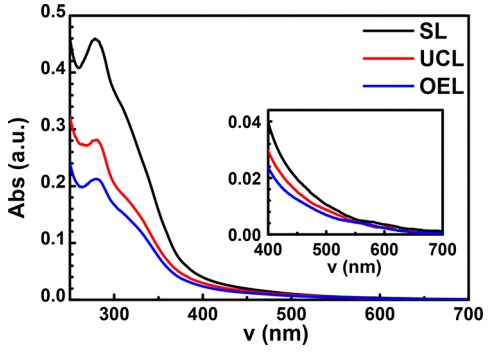

Figure 3. UV−vis spectra of neat SL, UCL, and OEL. The concentration of all samples in dioxane was 0.02 g/L. The inset highlights the absorption from 700 to 400 nm.

to neat SL, the absorptions of UCL and OEL in the UV region decreased significantly, and as evidenced in the inset shown in Figure 3, the absorption of the modified lignins within the visible region is also significantly reduced. It is known that the UV absorption of lignin arises principally from its conjugated phenolic groups,[39,40] as well as that the color of lignin may be lightened to some extent by the blocking of free-phenolic hydroxyl.[41] In this work, the esterification of SL consumed most of the phenolic hydroxyl groups and at the same time increased its overall molecular weight. Consequently, we observed a

DOI: 10.1021/acssuschemeng.7b02370
ACS Sustainable Chem. Eng. 2017, 5, 10342−10351

reduced absorption of the modified lignins in both UV and visible ranges, compared to neat SL at the same mass concentration in solution. The results from UV−vis spectra are in good accordance with NMR and FTIR results.

The thermal stabilities of neat and derivatized lignins (UCL and OEL) were investigated by TGA, and the results are shown in Figure 4. Compared to virgin lignin, the value of thermal

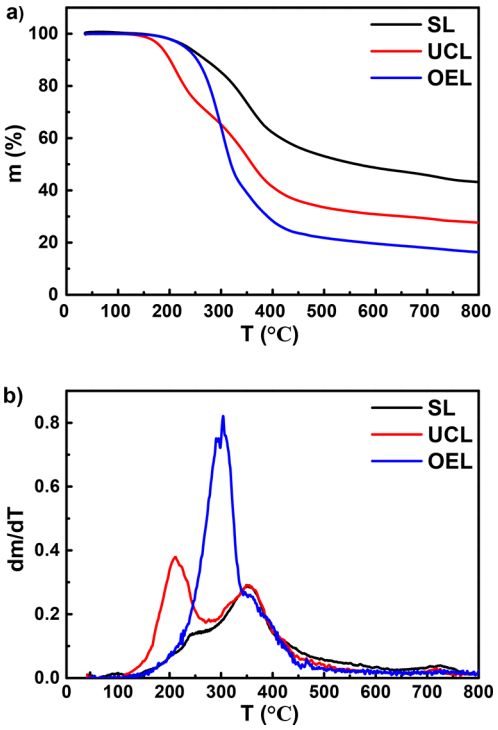

Figure 4. TGA (a) and DTA (b) curves of neat SL, 10-undecenoyl (UCL), and oleoyl (OEL) lignins.

parameter $T_{d,5}$ (calculated at mass loss of 5%) for oleoyl lignin remained almost unchanged (from 235.8 to 231.1 °C), but it markedly decreased for the undecenoyl one, at 183.9 °C (Figure 4a). In addition, the value of residual mass for lignin derivatives decreased to 29.1 and 17.9% for UCL and OEL, respectively, compared to 45.7% for untreated lignin.

The coupling of TGA with mass spectrometry was used for the determination of the species released during thermal degradation. The evolution of the total ion currents is given in the Supporting Information (Figures S1−S3). Both lignin derivatives degraded in two steps, with the shape of the differential thermogravimetry (DTG) curves varied with the nature of acyl side chains (Figure 4b). Common species were detected in the first degradation step such as ethylium ions (CH_2−CH_3+, m/z 29) and propenylium ions (CH_2═CH−CH_2+, m/z 41), indicating a probable degradation of the hydrocarbon chains. Additionally, CO_2 (m/z 44) was also detected. For the UCL, a strong signal of butenyl ions (CH_2═CH−CH_2−CH_2+, m/z 55) was also observed during this step.

The second degradation step for all the lignins in our study occurred at ∼360 °C, with mainly methylium ions (CH_3+, m/z 15) appearing on the spectra. Other signals including carbon monoxide and dioxide were also detected. This step corresponds to the demethylation of the lignin guayacyl and syringyl groups, which is independent of the chemical esterification modifications.

Differential scanning calorimetry (DSC) was used to study the effects on the glass transition temperature (T_g) provided by the two fatty acids grafted on SL. Generally, the T_g of lignin can be detected between 90 and 160 °C, depending on many factors such as the lignin origin, the molecular weight, or the corresponding extraction process.[42] Here, the T_g of SL was detected at 126 ± 2 °C, in good accordance with previous studies.[43] The OEL derivative possesses a lower T_g (103 ± 2 °C), as effect of the hydrogen-bond quenching (via esterification of the OH groups) and concomitant increase in free volume provided by oleoyl chains.[44] For UCL, the T_g spreads over a wide range of temperature and cannot be precisely detected (DSC traces are available in Figure S4).

Blends of Lignin Derivatives with PBAT. Neat SL and lignin derivatives (UCL and OEL) were melt-blended with PBAT at 10 and 20% loading, respectively, and the resulting composites were analyzed to investigate the influence of the modifications on their thermal, physical, and morphological properties.

SEM provides useful information about the morphology in the bulk surface of polymer compositions, as presented in Figure 5. It clearly shows that the untreated SL has limited compatibility with PBAT as large lignin aggregates (∼30−40 μm) are visible. As far as PBAT−UCL sample is concerned, reduced particle sizes (10−20 μm) are observed, confirming that the esterification of lignin with undecylenic acid enhances its compatibility with the PBAT matrix. The OEL also shows very fine particles (within 10 μm) within the cross-sectional surface; however, the zoomed-in part of Figure 5d displays some aggregations and existence of microvoids, indicating phase separation. The higher compatibility with PBAT observed for UCL compared to OEL could be attributed to the chemical similarity between the alkenyl ester substituents and the repeating butyrate−adipate units within the aromatic−aliphatic copolyester chains.

The mechanical properties of the PBAT−lignin composites were then evaluated through tensile testing at room temperature. From the stress−strain curves shown in Figure S5, it can be seen that all the materials had typical tensile behaviors for crystallizable ductile polymers, with yielding and necking followed by strain hardening. The results are summarized in Table 1. Neat PBAT films had a tensile strength (σ) of 29 MPa, tensile modulus (E) of 46 MPa, and elongation at break (ε) of 660%. The inclusion of SL into PBAT resulted in a clear change in its tensile properties. As reported in the literature, lignin with its amorphous 3D structure and the aromatic backbone, when blended with thermoplastic polymers, generally is able to enhance their strength and/or stiffness with the drawback of a significant drop of ductility.[45−48]

As expected, with the introduction of 10 wt % untreated lignin, a deterioration for both tensile strength and elongation at break was observed, as shown in Table 1. When the content of SL increased to 20 wt %, both parameters dramatically reduced to ∼14 MPa and 320%, respectively. In contrary, when blending 10 wt % UCL and OEL in PBAT matrix, the tensile strength remained almost unchanged compared to neat PBAT, and their elongation at break slightly improved. On the other hand, the Young's modulus dropped to 33.8 ± 4.2 and 20.1 ± 0.5 MPa, respectively, for UCL- and OEL-based composites due to the soft segments of lignin derivatives.[12] When the lignin derivatives content was increased to 20 wt %, both the tensile strength and elongation at break were reduced to some extent, but the values remained much higher than those of PBAT−SL composites. The better preservation of the tensile properties upon esterification

DOI: 10.1021/acssuschemeng.7b02370
ACS Sustainable Chem. Eng. 2017, 5, 10342−10351

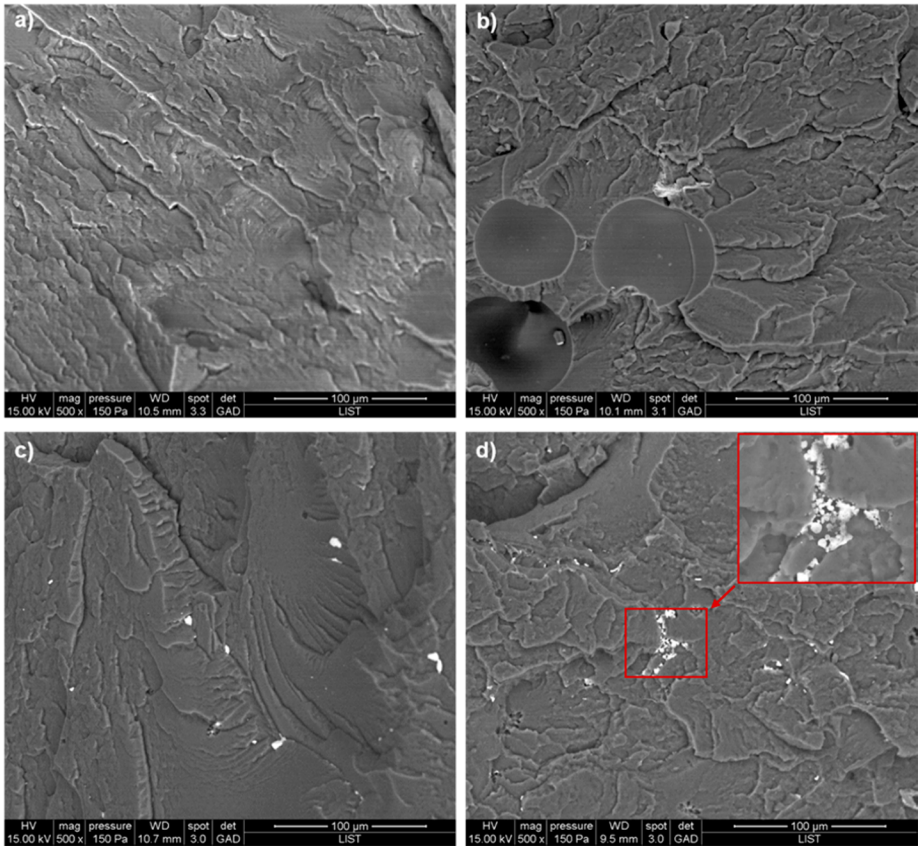

Figure 5. SEM images of cryo-fractures of PBAT (a), PBAT−SL blend (b), PBAT−UCL blend (c), and PBAT−OEL blend (d). All the blends contain 10 wt % of lignin or its derivative.

Table 1. Comparison of Tensile Properties of Various PBAT−Lignin Composite Films[a]

samples	ε elongation at break (%)	σ tensile strength (MPa)	E Young's modulus (MPa)
PBAT	655 ± 65.2	29 ± 3.8	46 ± 5.6
PBAT−SL-10%	418 ± 28.4	25 ± 2.4	63 ± 5.5
PBAT−UCL-10%	689 ± 51.4	29 ± 3.4	34 ± 4.2
PBAT−OEL-10%	679 ± 47.6	30 ± 3.4	20 ± 0.5
PBAT−SL-20%	322 ± 47.5	14 ± 1.2	62 ± 4.5
PBAT−UCL-20%	632 ± 76.6	26 ± 3.5	37 ± 5.0
PBAT−OEL-20%	522 ± 78.8	21 ± 4.1	23 ± 2.5

[a]Average values and standard deviation of 5−6 measurements per system.

can be ascribed to the presence of the hydrocarbon side chains, which exhibited a good compatibility with the PBAT matrix, leading to a better distribution of lignin derivatives in the composites. The stress-transfer was enhanced, which resulted in the increase of tensile strength and ductility values and the reduction in modulus. Similar results have also been reported with PE-esterified lignin composites.[30,49] Furthermore, by taking the standard deviations into account, the tensile test values did not significantly vary at a higher content of OEL and UCL, but slightly better tensile properties with the PBAT−UCL composites could still be observed due to higher compatibility for UCL with PBAT compared to OEL as discussed above. There is no doubt that lignin esterification provides significant improvement in the mechanical performances of PBAT composites compared to those with neat lignin material.

The thermal properties of the PBAT−lignin blends were then analyzed by TGA and DSC. TGA and DTG curves of neat PBAT and PBAT−(modified) lignin composites are shown in Figure 6. Thermal parameters $T_{d,5}$ and residual mass calculated at 700 °C are summarized in Table 2. It can be observed that PBAT exhibited the highest initial decomposition temperature ($T_{d,5}$ = 370 °C). The incorporation of lignins in PBAT resulted in lower $T_{d,5}$ (but still >300 °C with the exception of PBAT−OEL-20%), while neat PBAT possessed a higher mass loss rate, degrading in a narrower temperature range. With the exception of neat PBAT, the degradation of all the lignin composites can be divided into two steps. The first step was mainly associated with the degradation of lignins. The increase of acryl chain length and lignin content prompted the degradation. Because the mass percentage of oleoyl groups in OEL is higher than that of undecenoyl in UCL owing to more methylene/methine groups with oleoyl, and in addition the degradation of acyl chains occurs at lower temperature than the lignin skeleton, therefore PBAT−OEL-20% had the lowest $T_{d,5}$. The second degradation step was common to all materials and related to PBAT; however, the incorporation of lignins decreased the mass loss rate.

The DSC thermograms for neat PBAT and its lignin composites are illustrated in Figure 7, and the complete thermal data are summarized in Table 2. The incorporation of lignin into the PBAT matrix did not markedly affect the global degree of crystallinity (8.09−9.67 J·g^{-1}). However, it was observed that the

DOI: 10.1021/acssuschemeng.7b02370
ACS Sustainable Chem. Eng. 2017, 5, 10342−10351

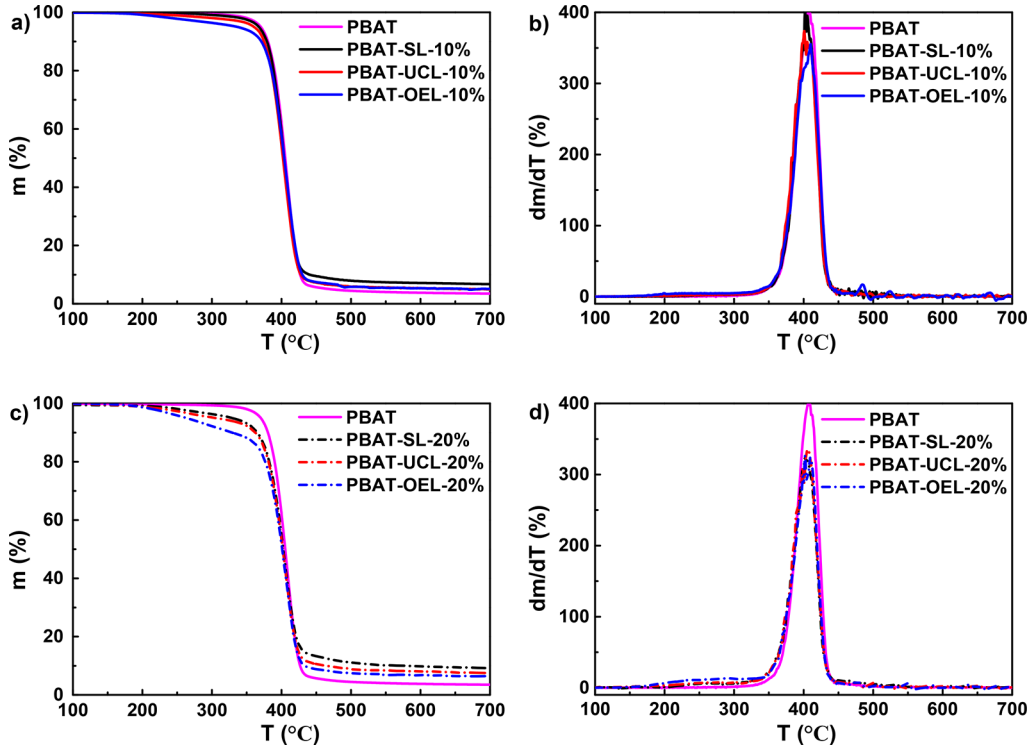

Figure 6. (a, c) TGA and (b, d) DTG curves of the as-prepared PBAT, PBAT−SL blends, PBAT−UCL blends, and PBAT−OEL blends. The blends contain (a, b) 10 or (c, d) 20 wt % of lignin.

Table 2. TGA and DSC Results of PBAT−(Modified) Lignin Composites

	TGA				DSC		
samples	$T_{d,5}$ (°C)	char (%)	T_c (°C)	ΔH_c (J/g)	T_g (°C)	T_m (°C)	ΔH_m (J/g)
PBAT	370.3	3.50	81.9	8.33	−33.3	119.5	5.72
PBAT−SL-10%	367.3	6.75	74.4	9.54	−29.5	117.1	6.09
PBAT−UCL-10%	360.5	4.98	77.1	9.42	−31.9	118.0	6.68
PBAT−OEL-10%	336.6	5.12	79.2	8.64	−37.9	117.5	6.17
PBAT−SL-20%	330.1	9.14	68.9	9.67	−26.6	115.6	7.53
PBAT−UCL-20%	304.7	7.53	81.8	8.69	−33.7	114.7	6.31
PBAT−OEL-20%	263.2	6.34	73.1	8.09	−38.7	114.4	5.86

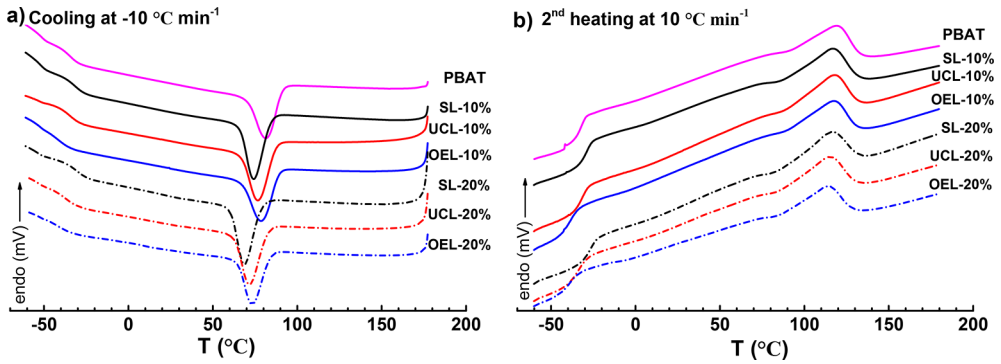

Figure 7. Cooling (a) and second heating (b) DSC curves of the as-prepared PBAT, PBAT−SL blends, PBAT−UCL blends, and PBAT−OEL blends. The blends contain 10 or 20 wt % of lignin.

initial T_c of PBAT shifted from 81.9 °C toward lower temperatures upon the addition of neat lignin to 74.4 °C at 10 wt % and 68.9 °C at 20 wt %. This result indicates that neat SL hindered the crystallization of PBAT to some extent, probably by restraining the movement of the polymeric chains. The T_m of PBAT blends slightly decreased, which seems to be influenced mostly by the lignin content rather than the varieties of (modified) lignins. The T_g of the PBAT blend with SL was slightly higher compared to neat PBAT. Such increase in T_g is most likely due to the abundance of rigid condensed phenolic structures and strong intermolecular hydrogen-bonding interactions in SL, which restrict the polymeric chain mobility.[50,51]

DOI: 10.1021/acssuschemeng.7b02370
ACS Sustainable Chem. Eng. 2017, 5, 10342−10351

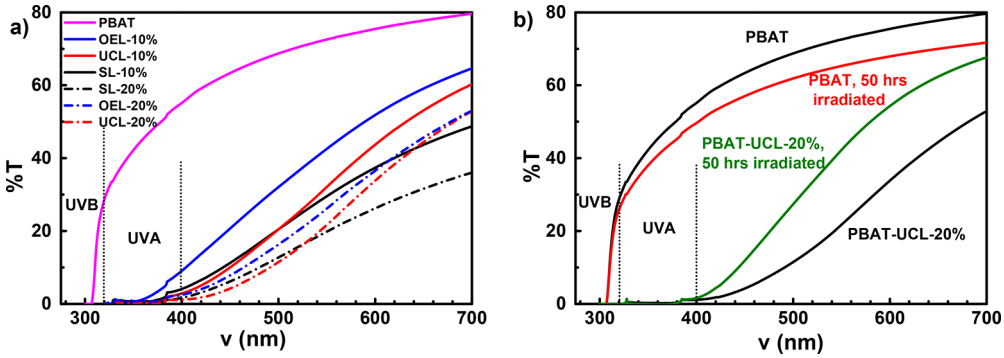

Figure 8. (a) Transmittance of the neat PBAT and PBAT−lignin composite films at different levels of lignin loading; (b) effects of UV irradiation on virgin PBAT and PBAT−UCL-20 wt % films on their light-transmittance behaviors.

The incorporation of the two modified lignins in PBAT triggered a more pronounced decrease of the T_g values, likely as a result of the soft fatty acid chains grafted onto the lignin. This result was particularly evidenced in composites with OEL and at higher lignin content.

The materials were then analyzed by UV−vis spectroscopy in order to investigate how the (modified) lignins affected the film UV-blocking capacity. The results of UV−vis characterization for neat PBAT and its lignin composite films (thickness normalized to 50 μm) before and after exposure under the UV light for 50 h are plotted in Figure 8. The neat PBAT films protected 92.3% of the UV−B light (280−320 nm) but had poor UV-barrier properties in the UV−A range (320−400 nm). All (modified) lignin−PBAT films exhibited much lower UV transparency, shading all of the UV−B and majority of UV−A. With 10 wt % lignin loading, the films had 97−99% of UV absorption in the UV−A range. The addition of 20 wt % lignin in the films further decreased the UV transmission and approached almost a complete block in the UV−A range. The UV-protection efficiencies of the PBAT-(modified) lignin films are comparable to the reported values for cellulose−lignin films[27] but superior to those for PLA−lignin,[28] nanocellulose−ZnO,[52] and nanocellulose−carbon dot composite films.[53] However, the transmittance of the produced composite films in the visible-light region was reduced (Figure 8a). The transparency of neat PBAT film was ∼73% (at 550 nm), while the transparency of films with 10 wt % lignin (29−43%) increased with the lengths of grafted chains in the modified lignins. For films with lignin content of 20 wt %, the transparency of the samples further decreased to 20−26%.

To investigate the effects of UV irradiation on the film's UV-protection stability, neat PBAT and PBAT−lignin composites were irradiated under UV using a xenon lamp for 50 h and then analyzed for the UV−vis light transmittance. Transmittance of neat PBAT film in UV−vis region was slightly decreased after UV exposure, due to the higher percentage of crystallinity in PBAT induced by the photodegradation.[54] Unexpectedly, the optical transparency of the PBAT−lignin composites increased significantly after exposure, particularly for PBAT−UCL-20% (Figure 8b and Figure S6). The discoloration of lignin can be attributed to two reactions. Under the UV exposure, phenolic hydroxyl groups in lignin generate phenoxyl radicals, which will turn into quinone structures. As quinones are efficient chromophores, their photo-oxidization into aliphatic acid structures will lead to blanching of SL.[55] The hydroperoxides generated during the photooxidation of PBAT matrix could serve as oxidizers needed in those reactions.[56] On the other hand, the UV-absorption capacity of the composite materials remained unchanged in the UV−B range and had slight reduction of UV absorption (93−98% of UV absorption) in the UV−A range, particularly for the films having 20 wt % lignin loading (>99% of UV absorption), suggesting that the films can withstand a relatively long UV exposure. These results clearly demonstrate that the incorporation of modified lignin in PBAT matrix can be applied to produce food packaging bags or agricultural materials, where UV-barrier property is mandatory.

CONCLUSIONS

In this study, soda lignin particles were modified by esterification reaction with 10-undecenoyl or oleoyl chlorides using 1.0 equiv with respect to total hydroxyl groups available at the lignin particle surface. The success of the reaction was confirmed by ^{31}P and ^{1}H NMR as well as FTIR spectroscopies. The undecenoyl-treated lignin was found to have a higher UV-absorption capacity but a lower thermal stability than the oleoyl-treated counterpart. To evaluate the potential of the modified lignin derivatives, they were blended with PBAT to produce thin films. The undecenoyl-treated lignin showed better compatibility with the PBAT matrix than the neat or oleoyl-grafted lignin, as revealed by SEM images. The introduction of 10 or 20 wt % lignin derivatives provided significant improvement in mechanical performances of the composites compared to those with neat lignin. Thermal analysis showed that, with the exception of 20 wt % oleoyl-grafted lignin, PBAT−lignin composites possessed good thermal stability ($T_{d,5}$ > 300 °C). The introduction of lignin derivatives in the PBAT film dramatically increased its UV-blocking properties, showing full absorption of UV light in 275−400 nm range. The composite films maintained the complete UV-absorption ability but enhanced the visible-light transparency even after the exposition to UV irradiation for 50 h. We proved that the grafting of biobased oleic or undecylenic acids onto soda lignin is a very promising tool to improve the compatibility of lignin with PBAT and to impart stable UV-blocking properties, while not negatively affecting (or even slightly improving) the PBAT mechanical properties. These biodegradable composite materials, with tunable optical, mechanical, and thermal properties could be exploited in the future for the production of food packaging bags or agricultural materials, where UV-barrier property is mandatory.

DOI: 10.1021/acssuschemeng.7b02370
ACS Sustainable Chem. Eng. 2017, 5, 10342−10351

■ ASSOCIATED CONTENT

Supporting Information

The Supporting Information is available free of charge on the ACS Publications website at DOI: 10.1021/acssuschemeng.7b02370.

TGA-MS spectra and DSC thermograms of the lignins, stress−strain curves for PBAT−lignin composite films and UV−vis spectra of the irradiated PBAT−lignin composite films (PDF)

■ AUTHOR INFORMATION

Corresponding Authors

*E-mail: philippe.dubois@list.lu.
*E-mail: wulinbo@zju.edu.cn.
*E-mail: wenjunwang@zju.edu.cn.

ORCID

Linbo Wu: 0000-0001-9964-6140
Wen-Jun Wang: 0000-0002-9740-2924

Notes

The authors declare no competing financial interest.

■ ACKNOWLEDGMENTS

Q.X., L.W., and W.-J.W. are grateful to the National Key Research and Development Program of China (2016YFB0302402) for financial support. P.D. thanks the Luxembourgish FNR for financial support in the frame of his PEARL chair.

■ REFERENCES

(1) Kaplan, D. L. Lignin. In *Biopolymers from renewable resources*; Springer: 1998; Chapter 12, pp 292−332.

(2) Werpy, T.; Petersen, G.; Aden, A.; Bozell, J.; Holladay, J.; White, J.; Manheim, A.; Eliot, D.; Lasure, L.; Jones, S. *Top value added chemicals from biomass. Volume 1: Results of screening for potential candidates from sugars and synthesis gas*; DTIC Document; Defense Technical Information Center: Fort Belvoir, VA, 2004.

(3) Bonawitz, N. D.; Chapple, C. The genetics of lignin biosynthesis: connecting genotype to phenotype. *Annu. Rev. Genet.* **2010**, *44*, 337−363.

(4) Constant, S.; Wienk, H. L.; Frissen, A. E.; de Peinder, P.; Boelens, R.; Van Es, D. S.; Grisel, R. J.; Weckhuysen, B. M.; Huijgen, W. J.; Gosselink, R. J.; et al. New insights into the structure and composition of technical lignins: a comparative characterisation study. *Green Chem.* **2016**, *18* (9), 2651−2665.

(5) *Monomers, Polymers, Composites from Renewable Resources*; Belgacem, M. N., Gandini, A., Eds.; Elsevier: New York, 2008.

(6) Xiao, B.; Sun, X.; Sun, R. The chemical modification of lignins with succinic anhydride in aqueous systems. *Polym. Degrad. Stab.* **2001**, *71* (2), 223−231.

(7) Stewart, D. Lignin as a base material for materials applications: Chemistry, application and economics. *Ind. Crops Prod.* **2008**, *27* (2), 202−207.

(8) Sen, S.; Patil, S.; Argyropoulos, D. S. Thermal properties of lignin in copolymers, blends, and composites: a review. *Green Chem.* **2015**, *17* (11), 4862−4887.

(9) Lora, J. H.; Glasser, W. G. Recent industrial applications of lignin: a sustainable alternative to nonrenewable materials. *J. Polym. Environ.* **2002**, *10* (1), 39−48.

(10) Laurichesse, S.; Avérous, L. Chemical modification of lignins: Towards biobased polymers. *Prog. Polym. Sci.* **2014**, *39* (7), 1266−1290.

(11) Ten, E.; Vermerris, W. Recent developments in polymers derived from industrial lignin. *J. Appl. Polym. Sci.* **2015**, *132* (24), 42069.

(12) Koivu, K. A.; Sadeghifar, H.; Nousiainen, P. A.; Argyropoulos, D. S.; Sipilä, J. Effect of Fatty Acid Esterification on the Thermal Properties of Softwood Kraft Lignin. *ACS Sustainable Chem. Eng.* **2016**, *4* (10), 5238−5247.

(13) Mariotti, N.; Hu, L.; Schorr, D.; Stevanovic, T.; Rodrigue, D.; Wang, X.-M.; Diouf, P. N.; Grenier, D. In *New bio-composites containing industrial lignins*; Proceedings of the 55th International Convention of Society of Wood Science and Technology, 2012; pp 1−9.

(14) Tinnemans, A.; Greidanus, P. Chemically modified lignin for the use in polymer blends. *Inst. Appl. Chem., TNO, Utrecht, Neth.* **1984**, 492−494.

(15) Pawar, S. N.; Venditti, R. A.; Jameel, H.; Chang, H.-M.; Ayoub, A. Engineering physical and chemical properties of softwood kraft lignin by fatty acid substitution. *Ind. Crops Prod.* **2016**, *89*, 128−134.

(16) Çalgeris, İ.; Çakmakçı, E.; Ogan, A.; Kahraman, M. V.; Kayaman-Apohan, N. Preparation and drug release properties of lignin−starch biodegradable films. *Starch-Stärke* **2012**, *64* (5), 399−407.

(17) Spiridon, I.; Teaca, C.-A.; Bodirlau, R. Preparation and characterization of adipic acid-modified starch microparticles/plasticized starch composite films reinforced by lignin. *J. Mater. Sci.* **2011**, *46* (10), 3241−3251.

(18) Rozite, L.; Varna, J.; Joffe, R.; Pupurs, A. Nonlinear behavior of PLA and lignin-based flax composites subjected to tensile loading. *J. Thermoplast. Compos. Mater.* **2013**, *26* (4), 476−496.

(19) Sahoo, S.; Misra, M.; Mohanty, A. K. Effect of compatibilizer and fillers on the properties of injection molded lignin-based hybrid green composites. *J. Appl. Polym. Sci.* **2013**, *127* (5), 4110−4121.

(20) Camargo, F. A.; Innocentini-Mei, L. H.; Lemes, A. P.; Moraes, S. G.; Durán, N. Processing and characterization of composites of poly (3-hydroxybutyrate-co-hydroxyvalerate) and lignin from sugar cane bagasse. *J. Compos. Mater.* **2012**, *46* (4), 417−425.

(21) Muthuraj, R.; Misra, M.; Mohanty, A. Hydrolytic degradation of biodegradable polyesters under simulated environmental conditions. *J. Appl. Polym. Sci.* **2015**, *132* (27), 42189.

(22) Södergård, A.; Stolt, M. Properties of lactic acid based polymers and their correlation with composition. *Prog. Polym. Sci.* **2002**, *27* (6), 1123−1163.

(23) Van de Velde, K.; Kiekens, P. Biopolymers: overview of several properties and consequences on their applications. *Polym. Test.* **2002**, *21* (4), 433−442.

(24) Kijchavengkul, T.; Auras, R.; Rubino, M.; Selke, S.; Ngouajio, M.; Fernandez, R. T. Biodegradation and hydrolysis rate of aliphatic aromatic polyester. *Polym. Degrad. Stab.* **2010**, *95* (12), 2641−2647.

(25) Glasser, W. G. In *Lignin: Historical, Biological, and Materials Perspectives*; Glasser, W. G., Northey, R. A., Schultz, T. P., Eds.; ACS Symposium Series; American Chemical Society: Washington, DC, 1999; Vol. *742*, pp 216−238.

(26) Nitz, H.; Semke, H.; Mülhaupt, R. Influence of lignin type on the mechanical properties of lignin based compounds. *Macromol. Mater. Eng.* **2001**, *286* (12), 737−743.

(27) Sadeghifar, H.; Venditti, R.; Jur, J.; Gorga, R. E.; Pawlak, J. J. Cellulose-Lignin Biodegradable and Flexible UV Protection Film. *ACS Sustainable Chem. Eng.* **2017**, *5* (1), 625−631.

(28) Chung, Y.-L.; Olsson, J. V.; Li, R. J.; Frank, C. W.; Waymouth, R. M.; Billington, S. L.; Sattely, E. S. A renewable lignin−lactide copolymer and application in biobased composites. *ACS Sustainable Chem. Eng.* **2013**, *1* (10), 1231−1238.

(29) Abächerli, A.; Doppenberg, F. Method for preparing alkaline solutions containing aromatic polymers. Canadian Patent CA2283698 A1, 1998.

(30) Buono, P.; Duval, A.; Verge, P.; Averous, L.; Habibi, Y. New insights on the chemical modification of lignin: acetylation versus silylation. *ACS Sustainable Chem. Eng.* **2016**, *4* (10), 5212−5222.

(31) Thiebaud, S.; Borredon, M. E.; Baziard, G.; Senocq, F. Properties of wood esterified by fatty-acid chlorides. *Bioresour. Technol.* **1997**, *59* (2), 103−107.

(32) Vaca-Garcia, C.; Borredon, M. Solvent-free fatty acylation of cellulose and lignocellulosic wastes. Part 2: reactions with fatty acids. *Bioresour. Technol.* **1999**, *70* (2), 135−142.

DOI: 10.1021/acssuschemeng.7b02370
ACS Sustainable Chem. Eng. 2017, 5, 10342−10351

(33) Argyropoulos, D. S. Quantitative phosphorus-31 NMR analysis of lignins, a new tool for the lignin chemist. *J. Wood Chem. Technol.* **1994**, *14* (1), 45−63.
(34) Granata, A.; Argyropoulos, D. S. 2-Chloro-4, 4, 5, 5-tetramethyl-1, 3, 2-dioxaphospholane, a reagent for the accurate determination of the uncondensed and condensed phenolic moieties in lignins. *J. Agric. Food Chem.* **1995**, *43* (6), 1538−1544.
(35) Duval, A.; Lange, H.; Lawoko, M.; Crestini, C. Reversible crosslinking of lignin via the furan−maleimide Diels−Alder reaction. *Green Chem.* **2015**, *17* (11), 4991−5000.
(36) Weng, F.; Li, X.; Wang, Y.; Wang, W. J.; Severtson, S. J. Kinetics and Modeling of Ring - Opening Copolymerization of l-Lactide and ε-Caprolactone. *Macromol. React. Eng.* **2015**, *9* (6), 535−544.
(37) Glasser, W. G.; Jain, R. K. Lignin derivatives. I. alkanoates. *Holzforschung* **1993**, *47* (3), 225−233.
(38) Olsson, S.; Östmark, E.; Ibach, R. E.; Clemons, C. M.; Segerholm, K.; Englund, F. The use of esterified lignin for synthesis of durable composites. In *7th Meeting of the Nordic-Baltic Network in Wood Material Science and Engineering (WSE)*, Oslo, 2011; pp 173−178.
(39) Falkehalg, S. I.; Marton, J. Chromophores in kraft lignin. In *Lignin Structures and Reactions*; Advances in Chemistry Series; American Chemical Society: Washington, DC, 1966; DOI: 10.1021/ba-1966-0059.fw001.
(40) Barsberg, S.; Elder, T.; Felby, C. Lignin-Quinone Interactions: Implications for Optical Properties of Lignin. *Chem. Mater.* **2003**, *15* (3), 649−655.
(41) Lin, S. Y. *Process for reduction of lignin color.* U.S. Patent No. US4184845, 1980.
(42) Glasser, W. G. Classification of lignin according to chemical and molecular structure. In *Lignin: Historical, Biological, and Materials Perspectives*; Northey, R. A., Glasser, W. G., Schultz, T. P., Eds.; American Chemical Society: Washington, DC, 2000. DOI: 10.1021/bk-2000-0742.ch009.
(43) Laurichesse, S.; Avérous, L. Synthesis, thermal properties, rheological and mechanical behaviors of lignins-grafted-poly (ε-caprolactone). *Polymer* **2013**, *54* (15), 3882−3890.
(44) Pu, G.; Hauge, D. A.; Gu, C.; Zhang, J.; Severtson, S. J.; Wang, W.; Houtman, C. J. Influence of Acrylated Lactide-Caprolactone Macromonomers on the Performance of High Biomass Content Pressure-Sensitive Adhesives. *Macromol. React. Eng.* **2013**, *7* (10), 515−526.
(45) Chen, F.; Dai, H.; Dong, X.; Yang, J.; Zhong, M. Physical properties of lignin-based polypropylene blends. *Polym. Compos.* **2011**, *32* (7), 1019−1025.
(46) Sailaja, R. Low density polyethylene and grafted lignin polyblends using epoxy-functionalized compatibilizer: mechanical and thermal properties. *Polym. Int.* **2005**, *54* (12), 1589−1598.
(47) Yue, X.; Chen, F.; Zhou, X. Improved interfacial bonding of PVC/wood−flour composites by lignin amine modification. *BioResources* **2011**, *6* (2), 2022−2044.
(48) Hilburg, S. L.; Elder, A. N.; Chung, H.; Ferebee, R. L.; Bockstaller, M. R.; Washburn, N. R. A universal route towards thermoplastic lignin composites with improved mechanical properties. *Polymer* **2014**, *55* (4), 995−1003.
(49) Dehne, L.; Vila Babarro, C.; Saake, B.; Schwarz, K. U. Influence of lignin source and esterification on properties oflignin-polyethylene blends. *Ind. Crops Prod.* **2016**, *86*, 320−328.
(50) Sarkanen, K. V.; Ludwig, C. H. *Liguins. Occurrence, formation, structure, and reactions.* Wiley-Interscience: New York, 1971.
(51) Wang, Y.; Xia, M.; Kong, X.; Severtson, S. J.; Wang, W.-J. Tailoring chain structures of l-lactide and ε-caprolactone copolyester macromonomers using rac-binaphthyl-diyl hydrogen phosphate-catalyzed ring-opening copolymerization with monomer addition strategy. *RSC Adv.* **2017**, *7* (46), 28661−28669.
(52) Jiang, Y. Q.; Song, Y. Y.; Miao, M.; Cao, S. M.; Feng, X.; Fang, J. H.; Shi, L. Transparent nanocellulose hybrid films functionalized with ZnO nanostructures for UV-blocking. *J. Mater. Chem. C* **2015**, *3*, 6717−6724.
(53) Feng, X.; Zhao, Y. F.; Jiang, Y. Q.; Miao, M.; Cao, S. M.; Fang, J. H. Use of carbon dots to enhance UV-blocking of transparent nanocellulose films. *Carbohydr. Polym.* **2017**, *161*, 253−260.
(54) Kijchavengkul, T.; Auras, R.; Rubino, M.; Ngouajio, M.; Fernandez, R. T. Assessment of aliphatic−aromatic copolyester biodegradable mulch films. Part I: Field study. *Chemosphere* **2008**, *71* (5), 942−953.
(55) Wang, J.; Deng, Y.; Qian, Y.; Qiu, X.; Ren, Y.; Yang, D. Reduction of lignin color via one-step UV irradiation. *Green Chem.* **2016**, *18* (3), 695−699.
(56) Cicchetti, O. Mechanisms of oxidative photodegradation and of UV stabilization of polyolefins. *Adv. Polym. Sci.* **1970**, *7*, 70−112.

DOI: 10.1021/acssuschemeng.7b02370
ACS Sustainable Chem. Eng. 2017, 5, 10342−10351